PCCP

Accepted Manuscript

This is an *Accepted Manuscript*, which has been through the Royal Society of Chemistry peer review process and has been accepted for publication.

Accepted Manuscripts are published online shortly after acceptance, before technical editing, formatting and proof reading. Using this free service, authors can make their results available to the community, in citable form, before we publish the edited article. We will replace this *Accepted Manuscript* with the edited and formatted *Advance Article* as soon as it is available.

You can find more information about *Accepted Manuscripts* in the **Information for Authors**.

Please note that technical editing may introduce minor changes to the text and/or graphics, which may alter content. The journal's standard **Terms & Conditions** and the **Ethical guidelines** still apply. In no event shall the Royal Society of Chemistry be held responsible for any errors or omissions in this *Accepted Manuscript* or any consequences arising from the use of any information it contains.

www.rsc.org/pccp

COMMUNICATION

Can electrodynamic interaction between molecule and metal dominate continuum background in surface-enhanced Raman scattering?

Mykhaylo M. Dvoynenko[a,c] and Juen-Kai Wang*[b,c]

A continuum background is always coincident with the Raman spectrum enhanced by metallic nanostructures and still remains elusive. Not only does it constitute a stymied mystery in the origin *per se*, but also reduces the useful quantifiable range of detection based on surface-enhanced Raman scattering (SERS). We examined theoretically near-field molecule-metal interaction to reveal its contribution to the SERS background. The results show that the spectral broadening of fluorescence and Raman scattering due to a nearby metal object is insignificant compared with experimental findings. This study abnegates the role of near-field interaction in the SERS continuum background and elucidates the microscopic molecule-metal electromagnetic interaction, despite being unable to pinpoint the primary source of SERS background.

1. Introduction

Surface-enhanced Raman scattering (SERS) has become a powerful analytic technique for assaying trace chemicals owing to emerging economical nanofabrication technologies, such as nanosphere lithography [1], anodic aluminium oxide [2], *etc*. The propitious Raman enhancers usually are made of ordered, nanometer-separated nanoparticle arrays [2]. For example, with the array of Ag nanoparticles embedded in nanochannels of anodic aluminium oxide, we have demonstrated high, uniform and reliable Raman enhancement and exploited it in assaying bacteria and their drug resistance [3] and lately in detecting Cu chlorophyll in vegetable oils [4]. Its optical idiosyncratics have been investigated with simulation [5], scattering spectroscopy [6], and near-field microscopy [7].

In spite of successful SERS-based detection examples, one common feature in measured SERS spectra is continuum background that would compromise the dynamical range of detection. The nature of the background is still stymied, though several models were proposed: fluorescence from metal nanoparticles [8] and inelastic

a. *V. Lashkaryov Institute of Semiconductor Physics, National Academy of Sciences of Ukraine, Kyiv, Ukraine.*
b. *Center for Condensed Mater Sciences, National Taiwan University, Taipei, Taiwan. E-mail: jkwang@ntu.edu.tw*
c. *Institute of Atomic and Molecular Sciences, Academia Sinica, Taipei, Taiwan.*

scattering of free electrons [9], *etc*. One interesting model proposed [10, 11] paid attention to the altered emitting characteristics of molecules in proximity of metal—dipole-image model. In that model, the reflection of the molecular Raman radiation from the nearby metal object was theorized to render the resultant Raman spectrum broadened owing to the damping dielectric response of metal. The aim of this work is to provide the theoretical analysis how the spectrum of the emitting molecule placed near a metal flat surface depends on the molecule-metal distance and the particle parameters (dielectric function and diameter). Through this analysis, the limits of the application of this dipole-image model to the SERS continuum background are portrayed. The effects of metal object are also discussed.

2. Fluorescent molecule near metal

The emitting spectrum of a molecule placed near a metal particle has been investigated with the use of both quantum [12] and classical [13, 14] approaches. This work follows a classical approach and considers both the spontaneous emission spectrum of a molecule near a metal sphere and the Raman spectrum of this composite system. Let us first consider a spontaneous radiating molecule—modelled as a dipole—in vacuum undertaking a harmonic oscillation along z axis. The electromagnetic wave emitted from this molecular dipole is scattered by a metal object; the scattered wave then acts on the oscillator. The equation of motion of the molecular dipole placed near the metal object can be written as

$$\frac{d^2z}{dt^2} + \gamma \frac{dz}{dt} + \omega_0^2 z = \frac{e^*}{m^*} E^{ref}(\vec{r}, t), \qquad (1)$$

where m^* is the effective mass of the dipole, γ is its radiation rate, ω_0 is its oscillating frequency, e^* is the effective electric charge of the dipole, and E^{ref} is the amplitude of the electric field reflected from the metal object. Note that γ can be interpreted by the action of the dipole on its self [15]. Looking for the solution of Eq. (1) in the form $z = z_0 e^{-i\omega t}$ for $E^{ref}(\vec{r}, t) = E^{ref}(\vec{r}, \omega)e^{-i\omega t}$, Eq. (1) becomes

$$-\omega^2 z_0 - i\gamma\omega z_0 + \omega_0^2 z_0 = \frac{e^*}{m^*} E^{ref}(\vec{r}, \omega). \qquad (2)$$

Since the total emitting field is proportional to the dipole ($e^* z_0$) and Eq. (2) is the equation for the eigen-frequency ω, the emitted spectra can be found. The reflected field is determined by

$$E^{ref}(\vec{r},\omega) = (k_0^2/\varepsilon_0)G_{zz}^{ref}(\omega,\vec{r},\vec{r})e^*z_0, \qquad (3)$$

where k_0 is the wavevector in vacuum, ε_0 is the vacuum permittivity, $G_{zz}^{ref}(\omega,\vec{r},\vec{r})$ is the zz component of the reflected part of the electrodynamic Green's tensor [14]. As a result, Eq. (2) can be rewritten as

$$\left[-\omega^2 - i\gamma\omega + \omega_0^2 - \frac{e^{*2}}{m^*}\frac{k_0^2}{\varepsilon_0}G_{zz}^{ref}(\omega,\vec{r},\vec{r})\right]z_0 = 0. \qquad (4)$$

Since the dipole moment is inversely proportional to $\left[-\omega^2 - i\gamma\omega + \omega_0^2 - \frac{e^{*2}}{m^*}\frac{k_0^2}{\varepsilon_0}G_{zz}^{ref}(\omega,\vec{r},\vec{r})\right]$, the emitted intensity I can be written as [12, 14]

$$I \propto \frac{\sum_{j=x,y,z}\cos^2\alpha_j\left|G_{jz}^0(\omega,\vec{r}_D,\vec{r})+G_{jz}^{ref}(\omega,\vec{r}_D,\vec{r})\right|^2}{\left|-\omega^2 - i\gamma\omega + \omega_0^2 - \frac{e^{*2}k_0^2}{m^*\varepsilon_0}G_{zz}^{ref}(\omega,\vec{r},\vec{r})\right|^2}, \qquad (5)$$

where $G_{jz}^0(\omega,\vec{r}_D,\vec{r})$ is the vacuum electrodynamic Green tensor, $\vec{r}_D$ is the position of the detector in far-field zone, α_j is the angle between the normal of the detector plane and $\vec{r}_D$. Both the vacuum $G_{jz}^0(\omega,\vec{r}_D,\vec{r})$ and reflected $G_{jz}^{ref}(\omega,\vec{r}_D,\vec{r})$ parts of the Green tensor are responsible for the transformation from the near-field zone to the far-field zone. The spectrum depends mainly on the denominator, but is slightly modified by the nominator.

Equations (4) and (5) can be analysed directly. Firstly, note that the emission spectrum can be modified due to the backscattering field (generalized radiation reaction force). The emitted spectrum is governed by the spectral behavior of $G_{zz}^{ref}(\omega,\vec{r},\vec{r})$. If the reflected part of the electrodynamic Green's function has no resonance near the eigen-frequency of the molecule in vacuum (ω_0), one can conclude that the real part of $G_{zz}^{ref}(\omega,\vec{r},\vec{r})$ is responsible for the Lamb shift: $\Delta\omega \approx \frac{e^{*2}k_0^2}{2m^*\varepsilon_0\omega_0}\text{Re}\left[G_{zz}^{ref}(\omega_0,\vec{r},\vec{r})\right]$, while its imaginary part alters the decay rate: $\gamma_{mod} = \gamma + \frac{e^{*2}k_0^2}{m^*\varepsilon_0\omega_0}\text{Im}\left[G_{zz}^{ref}(\omega_0,\vec{r},\vec{r})\right]$ [15]. These effects have been manifested by the spectral shift [16] of fluorescence and the huge decay rate for a fluorescent molecule placed near a metal surface [16, 17] and a moving plasma [18]. The dependence of the resonance frequency shift on the distance was experimentally demonstrated for Ag particles placed near a conducting surface [19]. The decrease of the molecule's fluorescence intensity, caused by the energy transfer to the metal surface, leads to a change of the ratio between Raman and fluorescence intensities [20] and was proposed to extract the enhancement factors of SERS [21] and to determine the fluorescence time [22] and molecule-metal distance [23]. If the resonance frequency ω_r of $G_{zz}^{ref}(\omega,\vec{r},\vec{r})$ is near ω_0, Eq. (3) can be considered as an equation of two coupled oscillators and can lead to Rabi splitting of the emitting spectra [14] and will be shortly discussed later.

Let us examine the spectral behavior in the case of a flat metal substrate and assume that ω_r is far from ω_0. The reflected part of the zz component of the Green function at the local response of the metal is [24]

$$G_{zz}^{ref}(\omega,\vec{r},\vec{r}') = \frac{1}{2\pi}\int_0^\infty dk_\parallel \frac{ik_\parallel^3(\varepsilon_2\eta_1-\varepsilon_1\eta_2)}{2k_0^2\varepsilon_1\eta_1(\varepsilon_2\eta_1+\varepsilon_1\eta_2)}e^{i\eta_1(z+z')}, \qquad (6)$$

where $\varepsilon_1 = 1$ and $\varepsilon_2 = \varepsilon_2' + i\varepsilon_2''$ are the dielectric functions of the vacuum and substrate, respectively, $k_\parallel$ is the wavevector component on the metal surface, $\eta_1 = \sqrt{\varepsilon_1 k_0^2 - k_\parallel^2}$, $\eta_2 = \sqrt{\varepsilon_2 k_0^2 - k_\parallel^2}$, z' is the molecule-metal distance, and z is the distance between the observation point and the molecule-metal system. If the both z and

z' are much less than the wavelength, the main contribution in the integral of Eq. (6) is given at high values of $k_\parallel \gg k_0$. Accordingly, $\eta_1 = \eta_2 = ik_\parallel$ and $G_{zz}^{ref}(\omega,\vec{r},\vec{r}')$ takes a mirror-image form [9, 11]

$$G_{zz}^{ref}(\omega,\vec{r},\vec{r}') = \frac{(\varepsilon_2-\varepsilon_1)}{2\pi k_0^2\varepsilon_1(\varepsilon_2+\varepsilon_1)}\frac{1}{(z+z')^3}. \qquad (7)$$

Equation (6) is obtained with the use of evanescent waves only and it is not valid for propagation waves. In other words, the image theory cannot by applied for the detection in far zone. This approximation is also called electrostatic approximation. With the use of Eq. (6), the frequency shift $\Delta\omega$ and the modified decay rate γ_{mod} are given below:

$$\Delta\omega \approx \frac{e^{*2}(\varepsilon_2'^2-\varepsilon_1^2+\varepsilon_2''^2)}{32\pi\varepsilon_1\varepsilon_0 m^*\omega_0[(\varepsilon_2'+\varepsilon_1)^2+\varepsilon_2''^2]z^3} \qquad (8)$$

and

$$\gamma_{mod} = \gamma + \frac{e^{*2}\varepsilon_1\varepsilon_2''}{8\pi\varepsilon_1\varepsilon_0 m^*\omega_0[(\varepsilon_2'+\varepsilon_1)^2+\varepsilon_2''^2]z^3}. \qquad (9)$$

Since $\gamma \propto \text{Im}[G_{zz}^0(\omega,\vec{r},\vec{r})]$ and $\gamma_{mod} \propto \text{Im}\left[G_{zz}^0(\omega,\vec{r},\vec{r}) + G_{zz}^{ref}(\omega,\vec{r},\vec{r})\right]$, Eqs. (8) and (9) can be rewritten as

$$\Delta\omega \approx \gamma\frac{3(\varepsilon_2'^2-\varepsilon_1^2+\varepsilon_2''^2)}{16k_0^3z^3\varepsilon_1^{3/2}\sqrt{\varepsilon_1}[(\varepsilon_2'+\varepsilon_1)^2+\varepsilon_2''^2]} \qquad (10)$$

and

$$\gamma_{mod} = \gamma\left[1 + \frac{3\varepsilon_2''}{4k_0^3z^3\sqrt{\varepsilon_1}[(\varepsilon_2'+\varepsilon_1)^2+\varepsilon_2''^2]}\right]. \qquad (11)$$

Equations (10) and (11) clearly show that the Lamb shift and spectral broadening strongly depend on the molecule-metal distance and how close the real part of the dielectric function of the metal (ε_2') to $-\varepsilon_1$. Note also that Eq. (10) indicates a possibility for both red and blue shifts depending on the value of ω_0 as regard to the frequency ω_r that is the frequency when $\varepsilon_2' = -\varepsilon_1$: Namely, $\Delta\omega < 0$, when $\varepsilon_2'^2 - \varepsilon_1^2 + \varepsilon_2''^2 \approx \varepsilon_2'^2 - \varepsilon_1^2 < 0$ for $|\varepsilon_2''| \ll \varepsilon_1$ and therefore $\omega_0 < \omega_r$; on the other hand, $\Delta\omega > 0$ when $\varepsilon_2'^2 - \varepsilon_1^2 + \varepsilon_2''^2 \approx \varepsilon_2'^2 - \varepsilon_1^2 > 0$ and $\omega_0 > \omega_r$. Let us consider two practical cases: The flat substrates are made of Au and Ag, $z = 1$ nm and the emitting wavelength is 560 nm. Taking a typical value of the radiation rate of $2 \times 10^8 \text{ sec}^{-1}$, $\Delta\omega \approx 3.4 \times 10^{13} \text{ sec}^{-1}$ (~5.7 nm) for Au and $\Delta\omega \approx 3.2 \times 10^{13} \text{ sec}^{-1}$ (~5.4 nm) for Ag. Furthermore, $\gamma_{mod} \approx 3.4 \times 10^{12} \text{ sec}^{-1}$ (~3.6 nm) for Au and $\gamma_{mod} \approx 8.6 \times 10^{11} \text{ sec}^{-1}$ for Ag (~0.9 nm). However, these spectral shifting and broadening are less than its inhomogeneous broadening, indicating that the influence of the metal substrate on the spontaneous radiation spectrum would be comparatively smaller with respect to the SERS continuum background. This principal conclusion remains even with the consideration of nonlocal response of metal [25-27]: The nonlocal consideration only alters line shifting and broadening slightly.

There is one situation in molecule-metal interaction altering the emitted spectrum dramatically: strong coupling between a single molecule and surface plasmon [14, 28-31]. The strong coupling was predicted [14, 28-31] at frequencies where the reflected part of the Green function has the resonance. Equation (7) shows that in the case of the flat substrate this frequency makes $\varepsilon_2' = -\varepsilon_1$. Equation (4) can be considered as an equation of two coupled oscillators and Rabi splitting can occur. For a silver particle such resonance condition takes place at UV, while for a gold particle Rabi splitting is insignificant because of a huge ε_2'' at $\varepsilon_2' = -\varepsilon_1$. However, even such dramatical change of the spontaneous radiation spectra cannot account for the broad SERS background happening at any excitation frequency. In sum, the theoretical analysis above shows that the spontaneous emission process of a molecule in proximity of a metal object cannot produce the continuum background observed in the SERS spectrum.

All formula and estimations considered above are valid for a flat substrate and for small molecule-metal distances. The decay rate, frequency shift and possible Rabi splitting are expected to be valid also in the case of a metal object with any shape if the molecule-metal distance is much smaller than its size. For example, for the molecule-metal distance of 1 nm the size of the metal object has to be approximately larger than 10 nm. Such conclusion was made with analytical consideration of the decay rate modification for a molecule near a spherical particle [32]. Accordingly, the portrayed frequency shift of fluorescence is not sensitive to the shape and the metal object as long as the molecule-metal distance is much less than the size of the metal object. Furthermore, since the local enhancement factor for the metal object differs from that of the flat surface in strength and wavelength dependence while with a comparable wavelength width, it modifies the intensity and the spectral shape of fluorescence in the former case.

It is natural to ask whether the inhomogeneous broadening per se will be enlarged and how it can be modified by the local enhancement factor. The origins of this inhomogeneous broadening are three folds: (1) variation in the molecule-metal distance, (2) variation in the particle shape and size, and (3) variation in the molecular orientation with respect to the metal surface. The variation of the molecule-metal distance can be due to the non-uniform thickness of the dielectric coating of the metal object, the differing adsorption orientations of an asymmetric molecule, *etc*. It can be varied from 0.5 to 5 nm. The upper bound of the induced spectral broadening is ~40 nm (for a dipole perpendicular to the metal surface) from Eq. (10) that is much smaller than the common SERS continuum background of >200 nm wide. Because the fluorescence quenching is active at short molecule-metal distances, the ultimate broadening is expected to be smaller than 40 nm. For the case of variation in particle shape and size, they only alter the spectral shape of fluorescence for a molecule at a specific distance from the particle, for example Ref. [33], thus without introducing more broadening. Finally, because the electromagnetic interaction between the dipole parallel to the metal surface is smaller than that between the dipole perpendicular, the frequency shift in the former case is smaller than 40 nm and this variation in the adsorption orientation of molecules also does not engender more broadening. In sum, these inhomogeneous sources ultimately only bring in extra spectral broadening of maximal 40 nm.

3. Raman scattering near metal

The focus of this study now falls upon the influence of the nearby metal object on the Raman process of the molecule. Contrary to the spontaneous emission, Raman scattering is coherently activated by the impinging light wave—videlicet, the Raman photon emits instantaneously with the excitation photon. The equation of motion for resonance Raman scattering of a specific vibrational mode may be written in framework of modulation theory [34] of Raman scattering by

$$\frac{d^2z}{dt^2} + \gamma\frac{dz}{dt} + \omega_0^2 z$$
$$= \frac{e^*(1+\Delta\cos\Omega t)}{m^*}\left[E_z^0(1+r^p)e^{-i\omega_i t} + E_z^{ref}(t)\right], \quad (12)$$

where E_z^0 is the amplitude of the z-component of the incident wave with an frequency ω_i, $E_z^{ref}(t)$ is the generalized radiation reaction force at all frequencies, and r^p is the Fresnel reflection coefficient. Contrary to Eq. (1), the dipole moment of the excited molecule in Eq. (12) is modulated by an amplitude Δ with a vibrational frequency Ω. As a note, Δ is proportional to the dynamical polarizability of the Raman process and is therefore less than unity. Accordingly, Eq. (12) is not an eigen equation and its solution generally consists of harmonic terms of ω_i, $\omega_i + \Omega$ and $\omega_i - \Omega$:

$$z = z_1 e^{-i\omega_i t} + z_2 e^{-i(\omega_i-\Omega)t} + z_3 e^{-i(\omega_i+\Omega)t}. \quad (13)$$

Substituting Eq. (13) into

$$E_z^{ref}(t) = \frac{k_0^2}{\varepsilon_0}G_{zz}^{ref}(\omega,\vec{r},\vec{r})e^*z(t) \quad (14)$$

gives $(1 + \Delta\cos\Omega t)E_z^{ref}(t) = \frac{k_0^2}{\varepsilon_0}G_{zz}^{ref}(\omega_i,\vec{r},\vec{r})e^*z_1 e^{-i\omega_i t}$

$+\frac{k_0^2}{\varepsilon_0}G_{zz}^{ref}(\omega_i-\Omega,\vec{r},\vec{r})e^*z_2 e^{-i(\omega_i-\Omega)t} + \frac{k_0^2}{\varepsilon_0}G_{zz}^{ref}(\omega_i+\Omega,\vec{r},\vec{r})$

$\times e^*z_3 e^{-i(\omega_i+\Omega)t} + \frac{\Delta}{2}\frac{k_0^2}{\varepsilon_0}G_{zz}^{ref}(\omega_i-\Omega,\vec{r},\vec{r})e^*z_1 e^{-i(\omega_i-\Omega)t}$

$+\frac{\Delta}{2}\frac{k_0^2}{\varepsilon_0}G_{zz}^{ref}(\omega_i+\Omega,\vec{r},\vec{r})e^*z_1 e^{-i(\omega_i+\Omega)t} + \frac{\Delta}{2}\frac{k_0^2}{\varepsilon_0}G_{zz}^{ref}(\omega_i,\vec{r},\vec{r})$

$\times e^*z_2 e^{-i\omega_i t} + \frac{\Delta}{2}\frac{k_0^2}{\varepsilon_0}G_{zz}^{ref}(\omega_i,\vec{r},\vec{r})e^*z_3 e^{-i\omega_i t}. \quad (15)$

Substituting the above equation and Eq. (13) into Eq. (12) produces three terms of the above three different frequencies: ω_i, $\omega_i + \Omega$ and $\omega_i - \Omega$. Equating their respective coefficients to zero leads to the following equations:

$$\left[-\omega_i^2 - i\gamma\omega_i + \omega_0^2 - \frac{e^{*2}}{m^*}\frac{k_0^2}{\varepsilon_0}G_{zz}^{ref}(\omega_i,\vec{r},\vec{r})\right]z_1 = \frac{e^*}{m^*}E_z^0(1+r^p) +$$
$$\frac{\Delta}{2}\frac{e^{*2}}{m^*}\frac{k_0^2}{\varepsilon_0}G_{zz}^{ref}(\omega_i,\vec{r},\vec{r})(z_2+z_3), \quad (16a)$$

$$\left[-(\omega_i-\Omega)^2 - i\gamma(\omega_i-\Omega) + \omega_0^2 - \frac{e^{*2}}{m^*}\frac{k_0^2}{\varepsilon_0}G_{zz}^{ref}(\omega_i-\Omega,\vec{r},\vec{r})\right]z_2 =$$
$$\frac{\Delta}{2}\frac{e^*}{m^*}E_z^0(1+r^p)\left[1 + e^*\frac{k_0^2}{\varepsilon_0}G_{zz}^{ref}(\omega_i-\Omega,\vec{r},\vec{r})z_1\right], \quad (16b)$$

and $\left[-(\omega_i+\Omega)^2 - i\gamma(\omega_i+\Omega) + \omega_0^2 - \frac{e^{*2}}{m^*}\frac{k_0^2}{\varepsilon_0}G_{zz}^{ref}(\omega_i+$
$\Omega,\vec{r},\vec{r})\right]z_3 = \frac{\Delta}{2}\frac{e^*}{m^*}E_z^0(1+r^p)\left[1 + e^*\frac{k_0^2}{\varepsilon_0}G_{zz}^{ref}(\omega_i+\Omega,\vec{r},\vec{r})z_1\right].(16c)$

Since $\Delta \ll 1$, $|z_2|,|z_3| \ll |z_1|$. Namely, Eq. (16a) is approximated as

$$\left[-\omega_i^2 - i\gamma\omega_i + \omega_0^2 - \frac{e^{*2}}{m^*}\frac{k_0^2}{\varepsilon_0}G_{zz}^{ref}(\omega_i,\vec{r},\vec{r})\right]z_1 \approx \frac{e^*}{m^*}E_z^0(1+r^p). (17)$$

The solutions of z_1, z_2 and z_3 are given by

$$z_1 \approx \frac{(e^*/m^*)E_z^0(1+r^p)}{-\omega_i^2 - i\gamma\omega_i + \omega_0^2 - \frac{e^{*2}k_0^2}{m^*\varepsilon_0}G_{zz}^{ref}(\omega_i,\vec{r},\vec{r})}, \quad (18a)$$

$$z_2 \approx \frac{\frac{\Delta}{2}\frac{e^*}{m^*}E_z^0(1+r^p)\left[1 + \frac{e^{*2}k_0^2}{m^*\varepsilon_0}\times\frac{G_{zz}^{ref}(\omega_i-\Omega,\vec{r},\vec{r})}{-\omega_i^2 - i\gamma\omega_i + \omega_0^2 - \frac{e^{*2}k_0^2}{m^*\varepsilon_0}G_{zz}^{ref}(\omega_i,\vec{r},\vec{r})}\right]}{-(\omega_i-\Omega)^2 - i\gamma(\omega_i-\Omega) + \omega_0^2 - \frac{e^{*2}k_0^2}{m^*\varepsilon_0}G_{zz}^{ref}(\omega_i-\Omega,\vec{r},\vec{r})}, \quad (18b)$$

and $z_3 \approx \frac{\frac{\Delta}{2}\frac{e^*}{m^*}E_z^0(1+r^p)\left[1 + \frac{e^{*2}k_0^2}{m^*\varepsilon_0}\times\frac{G_{zz}^{ref}(\omega_i+\Omega,\vec{r},\vec{r})}{-\omega_i^2 - i\gamma\omega_i + \omega_0^2 - \frac{e^{*2}k_0^2}{m^*\varepsilon_0}G_{zz}^{ref}(\omega_i,\vec{r},\vec{r})}\right]}{-(\omega_i+\Omega)^2 - i\gamma(\omega_i+\Omega) + \omega_0^2 - \frac{e^{*2}k_0^2}{m^*\varepsilon_0}G_{zz}^{ref}(\omega_i+\Omega,\vec{r},\vec{r})}. \quad (18c)$

Equations (13) and (18) are valid for both resonance and non-resonance Raman scattering and show that the metal object to the Raman scattering of a molecule in proximity alters its amplitude but not its Raman frequency. In other words, the near-field electromagnetic interaction between the molecule and the nearby metal object in the context of surface-enhanced Raman scattering only modifies its Raman intensity and does not introduce spectral broadening. This represents the first conclusion of the derivation.
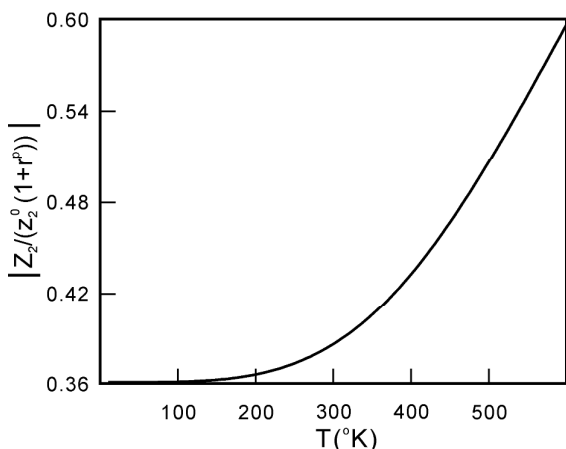
Figure 1. $|z_2/[z_2^0(1+r^p)]|$ calculated for a vibrational mode at 1650 cm^{-1} of rhodamine 6G placed 1 nm above a silver substrate as a function of temperature. The absorption peak is 530.5 nm and the excitation wavelength is 532 nm.

The similar conclusion was reached in an earlier work [35] without

consideration of a microscopic equation. The physical origin of this conclusion is that the resultant frequency of the Raman radiation of a specific vibrational mode is the outcome of the instantaneous frequency mixing between the excitation photon and the molecular vibration. In comparison, fluorescence is an emission process happening sporadically caused by the coupling between the emitting dipole and vacuum fluctuation [36].

The modification of the molecular Raman polarizability by the nearby metal object is then discussed below based on Eq. (18). First of all, the amplitude of the Raman scattering is modified by the factor $1+r^p$ that is the local enhancement factor in the case of a flat substrate and was investigated in the context of surface Raman spectroscopy [37]. However, there is additional factor associated with the near-field molecular-metal interaction that modifies the Raman polarizability [38]. Taking the Stokes radiation of Raman scattering as an example, Equation (18b) can be approximately rewritten as

$$z_2 \approx \frac{\frac{\Delta e^*}{2m^*}E_z^0(1+r^p)\left[1+\frac{2(\omega_i-\Omega)\Delta\omega+i\gamma_{mod}(\omega_i-\Omega)}{-\omega_i^2-i\gamma\omega_i+\omega_0^2-2\omega_i\Delta\omega-i\gamma_{mod}\omega_i}\right]}{-(\omega_i-\Omega)^2-i\gamma(\omega_i-\Omega)+\omega_0^2-2(\omega_i-\Omega)\Delta\omega-i\gamma_{mod}(\omega_i-\Omega)}, \quad (19)$$

while the corresponding vibration amplitude in the case of free space is given by

$$z_2^0 \approx \frac{\frac{\Delta e^*}{2m^*}E_z^0}{-(\omega_i-\Omega)^2-i\gamma_0(\omega_i-\Omega)+\omega_0^2}. \quad (20)$$

Note that the radiation rate for a molecule in free space γ_0 can be different from that close to the metal object γ. This is so because the molecule may undergo coupling with electrons and phonons of the metal object, which causes extra broadening [39]. In the case of non-resonant Raman process—$\gamma^2/[(\omega_i-\Omega)-\omega_0]^2 \ll 1$, the influence of the nearby metal object on the molecular Raman polarizability can be neglected according to Eq. (19). However, in the case of resonance Raman scattering, the influence of the nearby metal object on the Raman polarizability can be significant. For example, consider the molecule of rhodamine 6G with an absorption peak at 530.5 nm ($\omega_0 = 2\pi \times 5.66 \times 10^{16}$ rad/sec) that is placed 1 nm above a silver substrate and is excited at 532 nm ($\omega_i = 2\pi \times 4.96 \times 10^{15}$ rad/sec and a temperature dependent spectral broadening caused by electrons and phonons in the metal object—$\gamma \approx 208 \times (T/300)^2$ cm^{-1} [39], the dependence of $|z_2/[z_2^0(1+r^p)]|$ on temperature is presented in Fig. 1. For the sake of

simplicity the difference between values of γ_0 and γ is neglected. Here, the absorption peak is not influenced by temperature. Note that the polarizability of resonance Raman scattering is decreased by the nearby silver substrate with a factor ranging from 0.36 to 0.6 up to 500 K. Namely, the near-field molecule-metal interaction only slightly reduces the Raman signal slightly. This epitomizes the second conclusion of this part.

There indeed exist two mechanisms that can induce spectral broadening, as the molecule approaches a metal object. Firstly, the spectral width of a Raman peak is characteristic of its vibrational coupling with other degrees of freedom—turbulent electrons and vibration of atoms of metal. There have been many studies [40] in this physical mechanism. The induced spectral broadening is in the order of ~10 cm^{-1}. Secondly, the heterogeneous chemical interaction between the molecule and the metal at different surface sites (from weak charge-transfer interaction to structural change of molecule and to new bond formation) results in inhomogeneous broadening in the resultant Raman spectrum. According to the previous experimental works of molecular vibration at metal surfaces [41], the exhibited spectral broadening of the existing Raman peaks owing to such chemical interaction is at most ~10 cm^{-1}. The spectral broadening caused by these two mechanisms is certainly not large enough to account for the continuum background observed in surface-enhanced Raman scattering. Despite that Eqs. (18) and (19) were obtained for a flat metal surface, all conclusions are valid also for molecules near a metal object. In order to obtain Eq. (18) for the case of the metal object, it is just necessary to replace $1+r^p$ in Eq. (18) by corresponding local enhancement factor and the reflected part of the Green function by its corresponding function.

4. Conclusions

The near-field electromagnetic interaction between a molecule and a nearby metal object has been theoretically examined. Such interaction provides direct and reflected parts of fluorescence and Raman radiation, and the two together transpire weak damping and result in small spectral broadening. Two conclusions are reached in this work. Firstly, fluorescence of a molecule in proximity of a metal object bears approximately 5 nm (~120 cm^{-1} at 632.8 nm) broadening. Secondly, such spectral broadening does not repeat in the case of resonance Raman scattering owing to the instantaneous light-stimulated nature of Raman process. They are contrary to the conclusions of the two previous works [10, 11]. This study offers an opportunity to examine the contribution of near-field molecule-metal interaction to the SERS continuum background.

Acknowledgments

References

1   U. Ch. Fischer and H. P. Zingsheim, *J. Vac. Sci. Technol.*, 1981, **19**, 881; K. Hering, D. Cialla, K. Ackermann, T. Dörfer, R. Möller, H. Schneidewind, R. Mattheis, W. Fritzsche, P. Rösch, J. Popp, *Anal. Bioanal. Chem.*, 2008, **390**, 113.

2   H.-H. Wang, C.-Y. Liu, S.-B. Wu, N.-W. Liu, C.-Y. Peng, T.-H. Chan, C.-F. Hsu, J-K. Wang and Y.-L. Wang, *Adv. Mater., 2006,* **18**, 491.

3   T.-Y. Liu, K.-T. Tsai, H.-H. Wang, Y. Chen, Y.-H. Chen, Y.-C. Chao, H.-H. Chang, C.-H. Lin, J.-K. Wang and Y.-L. Wang, *Nat. Commun.*, 2011, **2,** 538.

4   W.-N. Lian, J. Shiue, H.-H. Wang, W.-C. Hong, P.-H. Shih, C.-K. Hsu, C.-Y. Huang, C.-R. Hsing, C.-M. Wei, J.-K. Wang and Y.-L. Wang, *Food Add. Contam.: Part A*, 2015, **32**, 627.

5   B.-Y. Lin, C.-H. Teng, H.-C. Chang, H.-H. Hsiao, J.-K. Wang, and Y.-L. Wang, *J. Sci. Comp.*, 2010, **45**, 429.

6   S. Biring, H.-H. Wang, J.-K. Wang, and Y.-L. Wang, *Opt. Express*, 2008, **16**, 15312.

7   T.-Y. Cheng, H.-H. Wang, S.-H. Chang, J.-Y. Chu, J.-H. Lee, Y.-L. Wang, and J.-K. Wang, *Phys. Chem. Chem. Phys.*, 2013, **15**, 4275.

8   G. T. Boyd, Z. H. Yu and Y. R. Shen , *Phys. Rev. B*, 1986, **33**, 7923; M. R. Beversluis, A. Bouhelier and L. Novotny, *Phys. Rev. B*, 2003, **68**, 115433.

9   Y. Maruyama and M. Futamata, *Chem. Phys. Lett.*, 2005, **412**, 65; Y. S. Ponosov and S. V. Streltsov, *Phys. Rev. B*, 2012, **86**, 045138.

10 S. Mahajan, R. M. Cole, J. D. Speed, S. H. Pelfrey, A. E. Russell, P. N. Bartlett, S. M. Barnett and J. J. Baumberg, *J. Phys. Chem. C*, 2010, **114**, 7242.

11 S. M. Barnett, N. Harris and J. J. Baumberg, *Phys. Chem. Chem. Phys.*, 2014, **16**, 6544.

12 C. Van Vlack, P. T. Kristensen, and S. Hughes, *Phys. Rev. B*, 2012, **85**, 075303.

13 J. J. Childs, K. An, R. R. Dasari, and M. S. Feld, *Cavity Quantum Electrodynamics*, ed. P. R. Barman, Academic Press, 1994, Chap. 8, 325.

14 M. M. Dvoynenko and J.-K. Wang, *Opt. Lett.*, 2013, **38**, 760.

15 E. A. Hinds, *Cavity Quantum Electrodynamics*, ed. P. R. Berman, Academic Press, 1994, Chap. 1, 1.

16 G. Cnossen, K. E. Drabe, and D. A. Wiersma, *J. Chem. Phys.*, 1993, **98**, 5276.

17 R. R. Chance, A. Prock and R. Silbey, *Adv. Chem. Phys.*, 1978, **37**, 1.

18 V. A. Kochelap and S. M. Kukhtaruk, *J. Appl. Phys.*, 2011, **109**, 114318.

19 W. R. Holland and D. G. Hall, *Phys. Rev. Lett.,* 1984, **52**, 1041.

20 P. Johansson, H. Xu and M. Käll, *Phys. Rev. B*, 2005, **72**, 035427.

21 M. M. Dvoynenko and J.-K. Wang, *Opt. Lett.*, 2007, **32**, 3552.

22 C. M. Galloway, P. G. Etchegoin and E. C. Le Ru, *Phys. Rev. Lett.*, 2009, **103**, 063003.

23 M. M. Dvoynenko, Z. I. Kazantseva, V. V. Strelchuk, O. F. Kolomys, E. F. Venger and J.-K. Wang, *Opt. Lett.*, 2010, **35**, 3808.

24 A. K. Zvezdin and V. I. Belotelov, *J. Opt. Soc. Am. B*, 2005, **22**, 228.

25 E. Castanie, M. Boffety, and R. Carminati, *Opt. Lett.*, 2010, **35**, 291.

26 R. Filter, C. Bosel, G. Toscano, F. Lederer, and C. Rockstuhl, *Opt. Lett.*, 2014, **39**, 6118.

27 S. Raza, S. Bozhevolnyi, M. Wubs, and N. Asger Mortensen, *J. Phys: Condens. Matter*, 2015, **27**, 183204.

28 N. S. Abadeer, M. R. Brennan, W. L. Wilson, and C. J. Murphy, *ACS Nano*, 2014, **8**, 8392.

29 A. Delga, J. Feist, J. Bravo-Abad, and F. J. Garcia-Vidal, *Phys. Rev. Lett.*, 2014, **112**, 253601.

30 S. D'Agostino, F. Alpeggiani, and L. C. Andreani, *Opt. Express*, 2013, **21**, 27602.

31 A. Delga, J. Feist, J. Bravo-Abad, and F. J. Garcia-Vidal, *J. Opt.*, 2014, **16**, 114018.

32 G. des Francs Colas, A. Bouhelier, E. Finot, J. C. Weeber, A. Dereux, C. Girard, and E. Dujardin, *Opt. Express*, 2008, **16,** 17654.

33 E. C. Le Ru, J. Grand, N. Felidj, J. Aubard, G. Levi, A. Hohenau, J. R. Krenn, E. Blackie, and P. G. Etchegoin, *Metal-Enhanced Fluorescence*, ed. C. D. Geddes. John Wiley & Sons, 2010, Ch. 2, p.25.

34 D. A. Long, *The Raman Effect*, Wiley, 2002.

35 F. W. King, R. P. Van Duyne, and G. C. Schatz, *J. Chem. Phys.*, 1978, 69, 4472; J. Gersten and A. Nitzan, *J. Chem. Phys.*, 1980, **73**, 3023.

36 P. W. Milonni, *The Quantum Vacuum. An Introduction to Quantum Electrodynamics*, Academic Press, 1994.

37 W. Suëtaka, *Surface Infrared and Raman spectroscopy*, Plenum Press, 1995.

38 M. Moskovits, *Rev. Mod. Phys.*, 1985, **57**, 783.

39 B. N. J. Persson and R. Ryberg, *Phys. Rev. B*, 1985, **32**, 3586.

40 O. M. Braun, A. I. Volokitin, and V. P. Zhdanov, *Sov. Phys. Usp.*, 1989, **32**, 605; R. G. Tobin, *Surf. Sci.*, 1987, **183**, 226; B. Hellsing and M. Persson, *Phys. Scipta*, 1984, **29**, 360; B. N. J. Persson and R. Ryberg, *Phys. Rev. B*, 1989, **40**, 10273.

41 Y. J. Chabal, *Surf. Sci. Rep.*, 1988, **8**, 211; S. Chiang, R. G. Tobin, P. L. Richards, and P. A. Thiel, *Phys. Rev. Lett.*, 1984, **52**, 648; H. Ueba, *Progr. Surf. Sci.*, 1986, **22**, 181; L.-W. Chou, Y.-R. Lee, J.-C. Jiang, J.-C. Lin, and J.-K. Wang, *J. Phys. Chem. C*, 2011, **115**, 516.